CHEMIJA. 2015. Vol. 26. No. 4. P. 244–253

Annealing effect on the structural and optical properties of black chromium electrodeposited from the Cr(III) bath

S. Survilienė*,

R. Juškėnas,

V. Jasulaitienė,

A. Selskienė,

A. Češūnienė,

A. Suchodolskis,

V. Karpavičienė

Center for Physical Sciences and Technology,
A. Goštauto St. 9,
LT-01108 Vilnius, Lithuania

Black chromium coatings were deposited on a steel substrate from the Cr(III) electrolyte containing ZnO as a second main component. The changes in the physical and optical properties of the sample owing to thermal degradation were examined by X-ray diffraction (XRD), transmission electron microscopy (TEM), X-ray photoelectron spectroscopy (XPS), scanning electron microscopy (SEM) and spectrophotometry. The coatings were annealed at a temperature of 600 °C in a nitrogen atmosphere for 2 hours to study the influence of annealing temperature on the structural, chemical and optical properties of black chromium. It has been found that the chromium solid solution in zinc of a hexagonal structure (*hcp*) along with that of zinc in chromium (*bcc*) may be formed during the electrodeposition of black chromium. The annealed black chromium was found to have dendrite-like ZnO and $ZnCr_2O_4$ particles of a crystalline structure and a small amount of Fe_2O_3, which is the result of oxidation of the steel substrate during the annealing process. Besides, a small quantity of iron atoms from the substrate was found to be incorporated into the $ZnCr_2O_4$ lattice. Therefore, the XRD patterns showed the presence of $FeCrZnO_4$. The analysis of the near-surface layers suggests that as-deposited black chromium is rich in hydroxides of both chromium and zinc and contains inclusions of metallic chromium, whereas after annealing of the sample the oxides become dominant in the absence of metallic Cr. The optical properties were characterized by the reflectance spectral measurements of the black coatings. The optical measurements have shown that the samples annealed at 600 °C exhibited a lower absorptivity compared to that for as-deposited black chromium, which depicted good absorptance properties for the absorption of solar energy. An increase in reflectance after annealing of the samples was found to be arising from the diffusion of the substrate material (Fe) into black chromium and the changes in the chemical composition and structure of the deposit. These findings confirm some of earlier observations and provide new information relating to the ability of black Cr–Zn coatings to collect solar energy.

Key words: solar selective black chromium, morphology, phase structure, optical properties

INTRODUCTION

Solar energy is usually absorbed by a black surface. Among solar selective coatings black chromium is widely used in solar collectors due to its high absorptivity in the visible and near infrared spectral regions, a good stability and a high thermal resistance [1, 2]. The black coatings which possess the high solar absorption ($\alpha \approx 0.9$) and low thermal emittance over the solar spectrum (0.3–2.5 μm) are effective selective coatings for the practical use [3]. Electroplated black chromium in combination with the metal substrate represents a solar selective absorber [4]. According to the data published

*Corresponding author: E-mail: sveta@ktl.mii.lt

[5–13], optical properties of black chromium are related to both the surface morphology and the amount of Cr_2O_3 in the black film which is made up of oxide and metallic phases. The morphology and structure of substrate were found to play an important role in the structure and thermal stability of the black chromium films [8]. It was shown [12] that the black chromium films containing 40–75% Cr_2O_3 possess the highest solar absorption. The action of elevated temperature on both the optical properties and lifetime of solar selective coating is discussed in the literature [14]. According to the published data [6] the degradation process of black chromium may be divided into two distinct phases: the first phase at lower and the second one at higher temperatures. Based on this, breakdown of chromium hydroxide to chromium oxide and H_2O takes place at temperatures under 300 °C, whereas oxidation of metallic chromium occurs during the second degradation phase (about 400 °C). The optical properties of black chromium on the steel substrate were found to remain excellent after being heat treated at 400 °C [13], whereas a stainless steel/black chromium system was stable even after heating at 450 °C [15]. Black chromium deposited on a copper substrate with a Ni undercoat was serviceable at temperatures under 350 °C [16]. An addition of Co^{2+} ions to the Cr(III) bath made it possible to improve both the color and absorption coefficient of black chromium [17]. According to the data published before [18], black chromium electrodeposited from the Cr(III)+ZnO bath, the phase structure of which may be classified as a solid solution, possessed good optical properties.

Our interest in electrodeposition of the Cr–Zn oxide coating resides in the search for a new material suitable for the use in solar thermal systems. The aim of this work was to deposit the black Cr-Zn coating and to evaluate the ability of such coating to collect solar energy. For this purpose we studied the action of annealing temperature on the structural, chemical and optical properties of black chromium.

EXPERIMENTAL

The black chromium coatings were electrodeposited on steel substrate containing 99.4% of iron, which was mechanically polished with further electropolishing before plating in accordance with the method given in [18]. A bath of a volume of 1 litre with two vertical Pt anodes and a cathode between them was maintained at a constant temperature (20 °C). The current density during plating was 0.2 and 0.4 A·cm^{-2}. The analytical grade chemicals (manufacturer Appli-Chem GMBH) and distilled water were used to prepare the plating bath containing chromium chloride, boric acid, sodium chloride, sodium nitrate, glycine (NH_2CH_2COOH) as a proper complexing agent for Cr(III) and zinc oxide as a second main component. The optimum composition of the plating bath is presented in Table 1. The quality of the deposit was assessed visually and by using an optical microscope. A deposit of good appearance and good adhesion was defined as appropriate for further research. The coatings were heat treated in flowing Ar (6.0) gas at 400 and 600 °C for 2 h.

The black chromium coatings were examined for the surface and cross sectional morphology and chemical composition using scanning electron microscopy (SEM) and energy disperse spectroscopy (EDS), respectively. In order to choose a typical picture for each coating, three–four locations (in the central zone) were taken. The SEM characterization of black chromium surface morphology, focused ion beam (FIB) prepared cross-sections and EDX analysis were carried out in a dual beam system FE-SEM-FIB Helios Nanolab 650 (FEI Company) equipped with an X-ray spectrometer X-Max (Oxford Instruments). The TEM measurements were conducted with a Tecnai G2 F20 X-TWIN (FEI Company).

Table 1. **The base composition of the black Cr(III) bath**

Component	G dm^{-3}
$CrCl_3$ $6H_2O$	250
NH_2CH_2COOH	18.75
H_3BO_3	30.0
NaCl	60.0
$NaNO_3$	3.0
ZnO	5.0–10.0
pH = 1.2	
Temperature 20 °C	
i_c = 0.2–0.4 A cm^{-2}	

The phase composition of black chromium was examined by using X-ray diffraction (XRD). The XRD studies were conducted using an X-ray diffractometer Smart Lab (Rigaku) equipped with a 9 kW rotating Cu anode X-ray tube. The grazing incidence (GIXRD) method was used in the 2θ range 30–75°. The angle between the parallel beam of X-rays and the specimen surface (w angle) was adjusted to 0.5°.

Elemental analysis of the coatings and the valence state of elements were studied using XPS. The spectra were recorded with a Vacuum Generator (VG) ESCALAB MK II spectrometer. The non-monochromatic Al K_α X-ray radiation ($h\nu$ = 1 486.6 eV) was used for excitation. The Al twin anode was powered at 14 kV and 20 mA. The photoelectron take-off angle was 45° with respect to the sample surface normal and spectra of Cr2p, Zn2p, O1s, C1s and N1s were taken at the constant analyzer energy mode (20 eV pass energy). The base pressure was kept below 5×10^{-8} Torr in the working chamber. The spectrometer was calibrated in reference to Ag3d5/2 at 368.0 ± 0.1 eV and Au4f7/2 at 83.8 ± 0.1 eV. XPS depth profiling was performed in the preparation chamber where the argon gas pressure was maintained at 6×10^{-5} Torr with a 50 l/s pumping speed at the gauge. Every time after sputtering the specimen was carried immediately to the analyzer chamber to avoid the rest gas adsorption. The quantitative elemental analysis was performed by determining peak areas and taking into account empirical sensitivity factors for each element [19, 20]. A standard program was used for data processing (XPS

spectra were treated by Shirley-type background subtraction and fitted with mixed Gaussian–Lorentzian functions).

Spectral reflectance measurements were used to investigate the optical selectivity of samples coated with black chromium. Relative diffusive and specular reflection spectra were measured in a Shimadzu UV-3600 two beam spectrometer equipped with a multi-purpose compartment MPC-3100 by means of an integrating sphere of the 60 mm diameter coated by barium sulphate. Also the barium sulphate target was used as a diffusive reflective standard.

RESULTS AND DISCUSSION

It was found that an increase in both current density and zinc concentration in the Cr(III) bath gave rise to zinc percentage in the deposit (Fig. 1). The influence of zinc on the surface morphology is shown in Fig. 2. It is seen that the higher

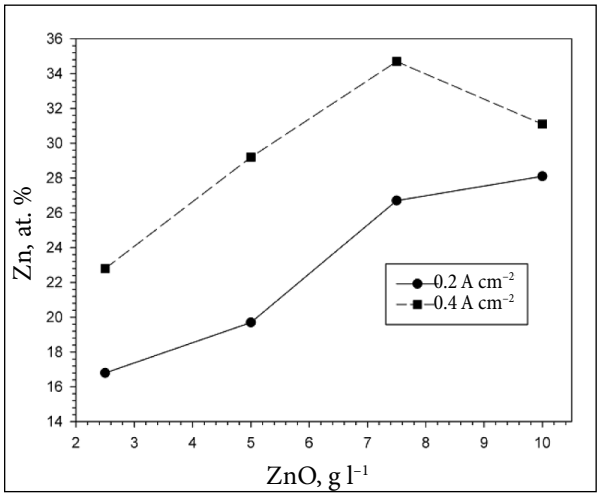

Fig. 1. Percentage of zinc in the black chromium coating as a function of ZnO concentration in the Cr(III) bath

the ZnO concentration in the Cr(III) bath, the smoother the surface of the coating obtained under the same electrolysis conditions (compare samples "a" with "b" and "c" with "d"). A loose structure with a dark "vein-like" network of cracks and a large number of globular particles is observed in the coating deposited from the bath with a low ZnO content (samples "a" and "c"). Close examination of some large particles revealed that they are agglomerations of very fine particles. The dimensions of agglomerations are about 1.0 to 3.0 μm in diameter among which 1.8 μm is dominant. These agglomerations consist of a large number of very fine particles (about 0.3 μm), which appear to be surrounded by some amorphous oxides and hydroxides.

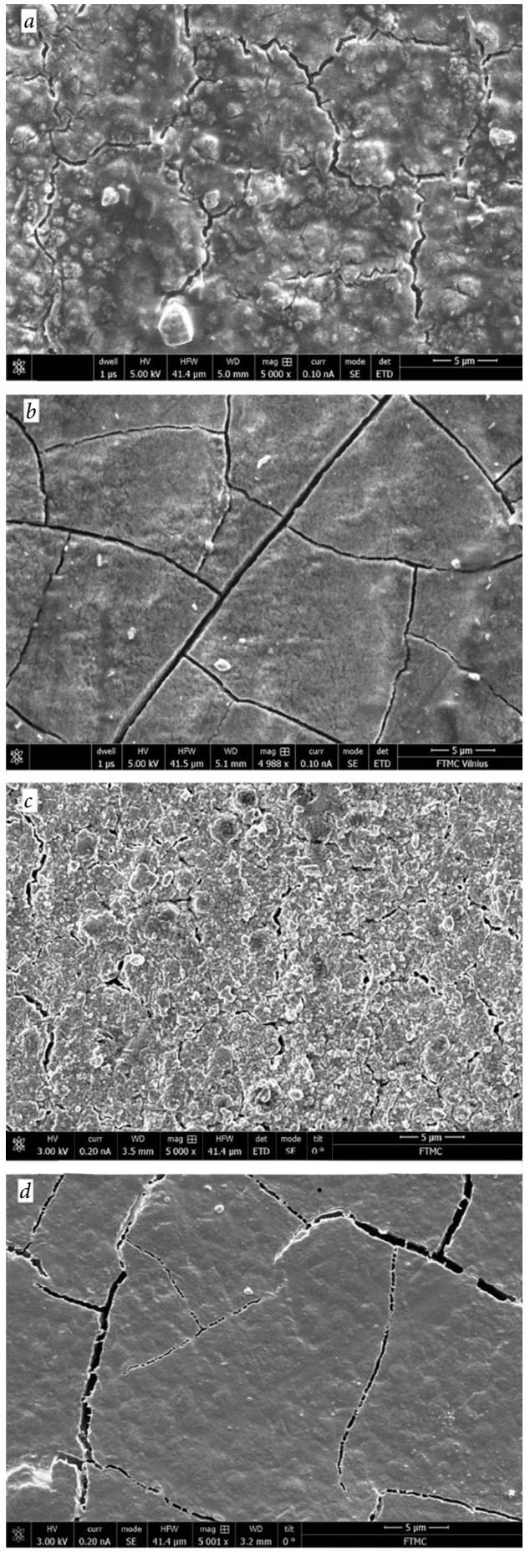

Fig. 2. Surface morphology of black chromium electrodeposited from the Cr(III) bath containing ZnO: 2.5 g l^{-1} (*a*), 5.0 g l^{-1} (*c*) and 10.0 g l^{-1} (*b*, *d*) at 0.2 A cm^{-2} (*a*, *b*) and 0.4 A cm^{-2} (*c*, *d*)

In order to identify the predominant chromium phase in the deposited layer, the deposits were investigated using an X-ray diffractometer (XRD) before and after annealing. XRD patterns of as-deposited Cr–Zn layers (Fig. 3) demonstrate two kinds of peaks: the sharp one, which is assigned to the steel substrate and broad peaks at lower angles suggesting the same body centered cubic structure (*bcc*), however, with a larger lattice parameter. The lattice parameter of α-Fe equals 0.28664 nm (# 00-006-0696), that of Cr is 0.28839 nm (# 00-006-0694) and the broad XRD peaks correspond to the *bcc* structure with the lattice parameter of about 0.298 nm for the coating containing 12.24 at.% of Zn. The latter lattice parameter increases up to 0.299 nm as the amount of Zn reaches about 16.68 at.%. These results suggest that the abovementioned *bcc* structure is a Zn solid solution in chromium, the lattice parameter of which increases with the Zn amount. It should be pointed out that the increase in Zn amount leads to the emergence of additional peaks which are attributable to the hexagonal structure characteristic of metallic zinc though with a bit different lattice parameters a = 0.268 and c = 0.484 nm instead of a = 0.2665 and c = 0.4947 nm (according to ICDD data base card # 00-004-0831). This implies that the chromium solid solution in zinc of a hexagonal structure (*hcp*) was formed along with that of zinc in chromium (*bcc*).

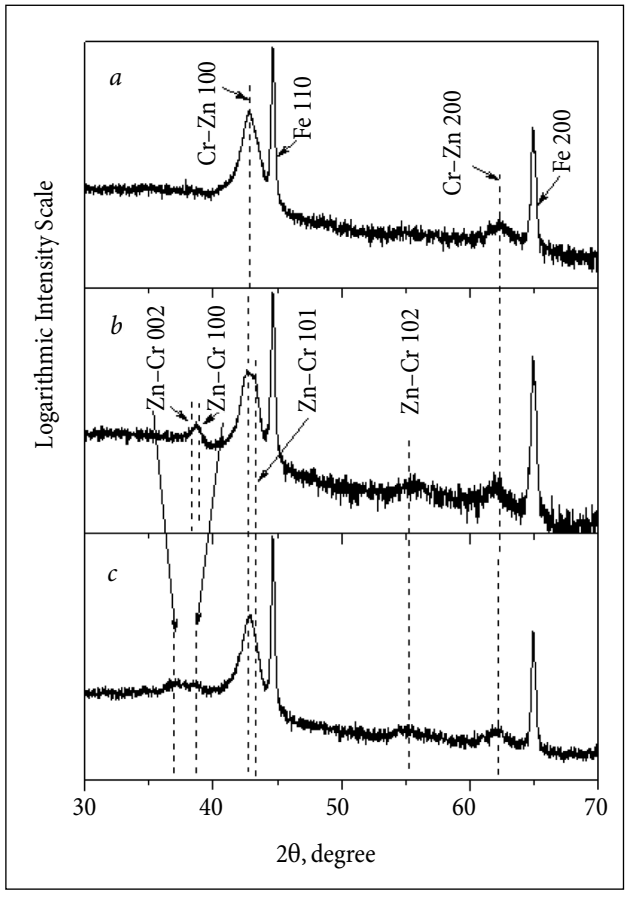

Fig. 3. XRD patterns of as-deposited black chromium at i_k = 0.4 A cm^{-2} from the Cr(III) bath containing ZnO: 5 g l^{-1} (*a*), 10 g l^{-1} (*b*) and 7.5 g l^{-1} (*c*)

Figure 4 shows a focused ion beam (FIB) made cross-section image of the Cr–Zn layer which points to the fact that the Cr–Zn layer represents dendrite-like metallic structures (lighter parts of the Cr–Zn layer) in the matrix of different material (darker parts of layer). Dendrite-like formations

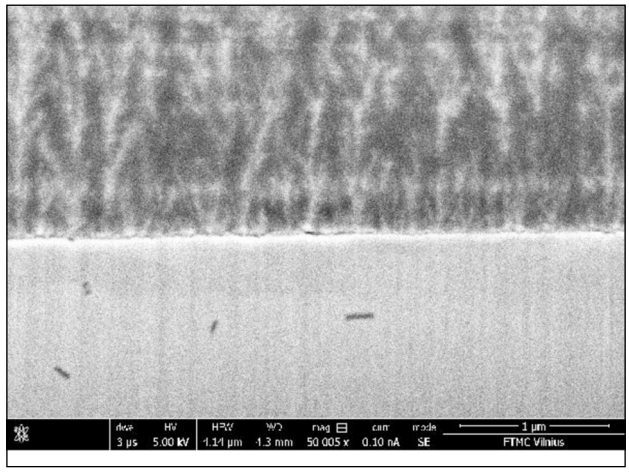

Fig. 4. SEM cross-section image of the Cr–Zn layer (darker part) on the steal substrate (light grey part)

are of too small dimensions to be examined by EDX in SEM. That is why TEM was employed to determine the origin of these formations. Figure 5a depicts a TEM image of FIB cut lamella of the Cr–Zn layer cross-section. The TEM image corroborates the presence of dendrite-like formations in the matrix of a lighter material. Electron diffraction images taken from the place without formations (ED_1) and from the place with dendrites (ED_2) are shown in Fig. 5b and c, respectively. The ED_1 shows a broad amorphous ring only, while ED_2 depicts white spots characteristic of the crystalline structure with the *bcc* crystal lattice and the lattice parameter being of about 0.3 nm. Most likely the dendrite-like formations present a substitution solid solution of Zn in chromium established by the XRD measurements.

According to the literature data [13], diffusion of the substrate material and optical degradation may occur in the black chromium/substrate system at a temperature of about 400 °C. However, our thermal stability test (at 400 °C) did not cause the appearance of any new characteristic features in the XRD patterns, which suggests that the samples under study were stable at temperatures up to 400 °C. Figure 6 shows the XRD patterns of the Cr–Zn coatings annealed at a temperature of 600 °C for 2 hours in the Ar (6.0) atmosphere. The pattern analysis discloses that the annealed coatings are composed of $FeCrZnO_4$ (# 00-043-0554) and ZnO (# 01-089-0511). One sharp but rather weak peak, which emerged at the diffraction angle of about 44.2°, is not attributable to any oxide and may be assigned to the *bcc* structure characteristic of the Zn solid solution in chromium. The lattice parameter of the *bcc* structure in the annealed layers equals 0.290 nm. A small amount of Fe_2O_3 (Hematite, # 00-033-0664) and Fe_2O_3 (Magnetite, #

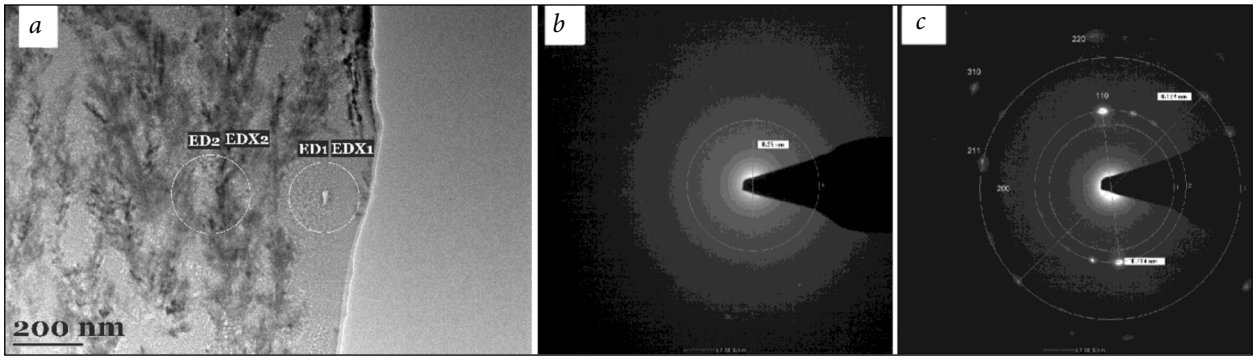

Fig. 5. TEM image of the Cr–Zn layer deposited from the Cr(III) bath containing 5 g dm^{-3} ZnO: cross-section (*a*) and electron diffractograms from the areas indicated in the cross-section image as ED_1EDX_1 (*b*) and ED_2EDX_2 (*c*)

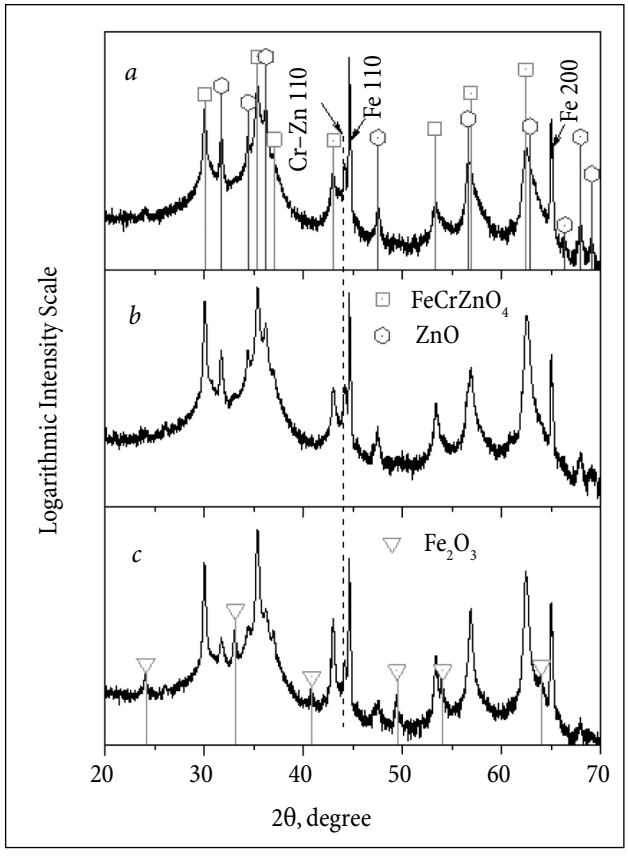

Fig. 6. XRD patterns of the Cr–Zn coatings deposited on the steel substrate and annealed at temperature of 600 °C in Ar (6.0) atmosphere for 2 h, where Cr–Zn 110 indicates the peak of bcc structure. The coatings contain 12.24 at% Zn (*a*), 13.53 at% Zn (*b*) and 16.68 at. % Zn (*c*)

00-039-1346) is present in the annealed Cr–Zn sample containing the largest quantity of Zn and possessing the lowest thickness (Fig. 6c). It is likely that these oxides are the result of oxidation of the steel substrate surface during the annealing process. Since the annealing of samples was conducted under the pure argon (6.0) atmosphere, the oxidation of the steel surface should took place due to oxygen which is present in the as-deposited Cr–Zn coating (Table 2). It is known [1] that the diffusion of the substrate material (Fe) into black chromium plays a major role in solar absorption decrease. Besides, the change in the chemical composition of the selective coating, which may be caused by oxidation of the metallic chromium, is also responsible for a decrease in solar radiation absorption.

Table 2. **The atomic percentages of zinc, chromium and oxygen in black chromium deposited at 0.4 A cm^{-2} from the Cr(III) bath containing ZnO**

Sample No.	ZnO in bath, g dm^{-3}	Zn, at.%	Cr, at.%	O, at.%
1.	5	12.24	16.85	69.44
2.	7.5	13.53	15.12	70.25
3.	10	16.68	13.00	68.90

SEM images of the surface of the annealed Cr–Zn layers are shown in Fig. 7. The width of cracks seems to be wider in the layers with a higher Zn quantity. Thin white plates are seen in the cracks of the Cr–Zn layer with the lowest Zn quantity (Fig. 7b) and there are no such plates in the cracks of the layer with the largest quantity of Zn (Fig. 7c).

The EDX technique was employed to determine the origin of the plates. Table 3 presents the chemical composition of the surface areas indicated in Fig. 8(a) as Spectrum 1 and Spectrum 2. Spectrum 1 was taken from the crack containing thin plates, and Spectrum 2 was taken from the Cr–Zn layer. The crack (Spectrum 1) contains a significantly larger quantity of Zn as compared to that of Cr. The thin white plates are ZnO. The latter conclusion is corroborated by the measurement of Cr–Zn layers with low and the largest quantities of Zn (Spectrum 2 in Table 3). Figure 8(b) shows that there are no thin white plates in the cracks and indeed the area of Spectrum 1 contains a very small amount of Zn (Table 3b).

On the other hand, the chemical composition of the areas of Spectrum 2 in all cases suggests that $ZnCr_2O_4$ is present in the annealed Cr–Zn layer instead of $FeCrZnO_4$ marked in Fig. 6. However, the lattice parameters of the compounds differ significantly: 0.8327 nm for $ZnCr_2O_4$ (# 00-022-1107) and 0.8396 nm for $FeCrZnO_4$. Since the diffractometer was tested with the LaB_6 standard (RSM 660b from NIST), this

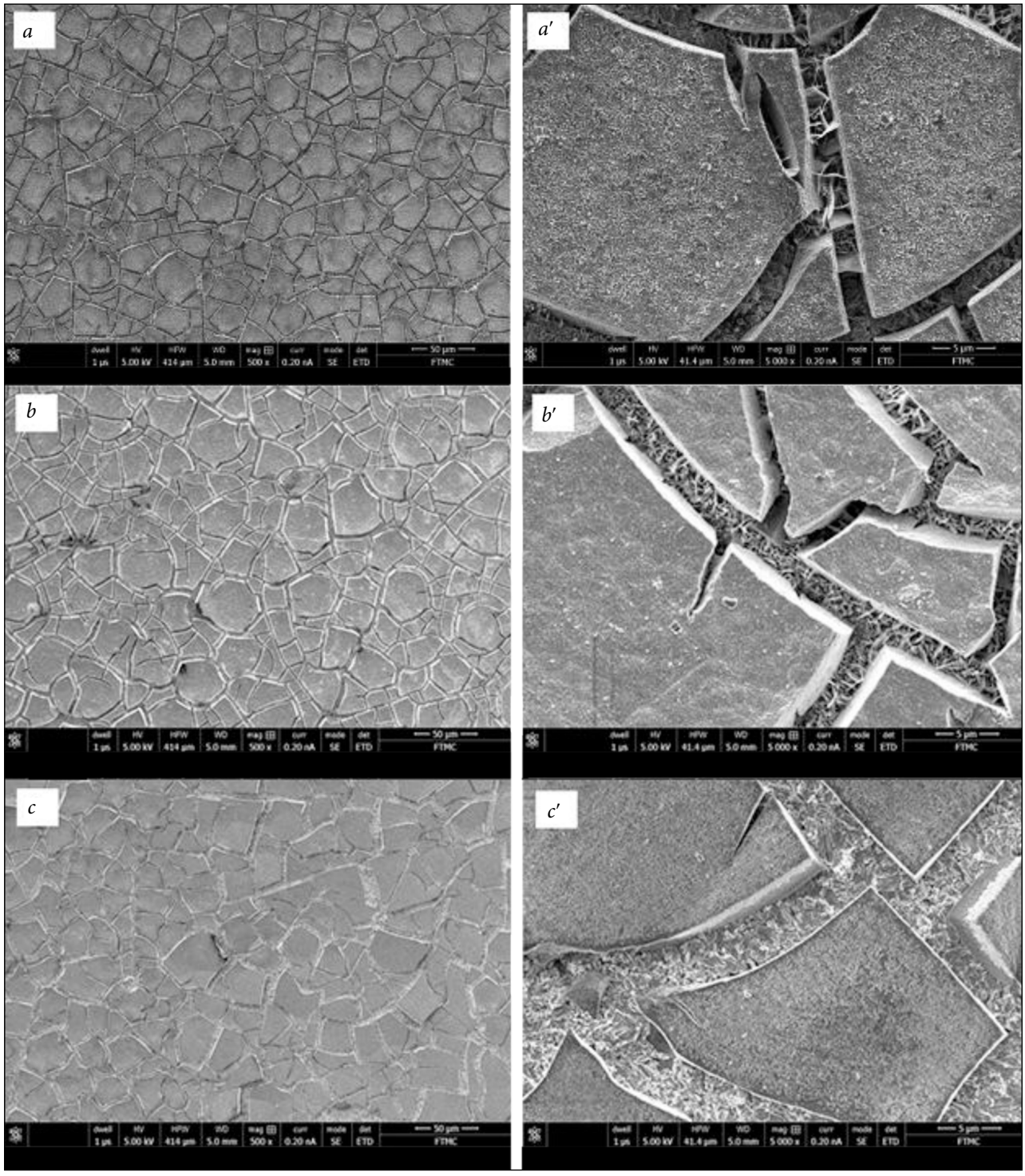

Fig. 7. SEM images of the annealed Cr-Zn layers deposited from Cr(III) baths containing ZnO (g dm^{-3}): *a* – 5.0; *b* – 7.5; *c* – 10.0

Table 3. **Chemical composition (at%) in different areas of annealed Cr–Zn coatings deposited from Cr(III) baths containing ZnO: 5.0 g dm^{-3} (a) and 10.0 g dm^{-3} (b)**

Surface area	O	Mg	Cl	Ca	Cr	Fe	Zn
a) Spectrum 1	14.3	0	0.22	0.01	7.64	61.18	16.65
Spectrum 2	63.85	0.18	1.54	0.56	18.27	1.13	14.47
b) Spectrum 1	61.11	0.01	0.02	0.04	0.84	37.09	0.89
Spectrum 2	63.54	0.11	1.26	0.1	15.04	1.46	18.48

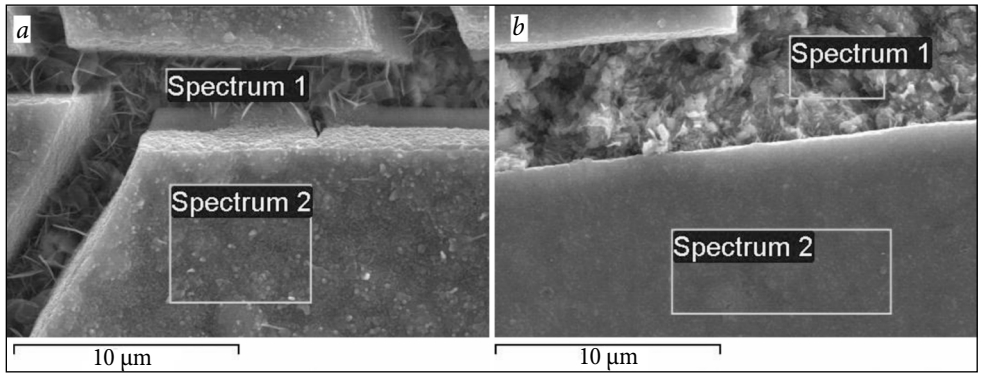

Fig. 8. SEM images of the annealed Cr–Zn layers deposited from Cr(III) baths containing 5.0 g dm^{-3} ZnO (*a*) and 10.0 g dm^{-3} (*b*)

cannot be a measurement error. So the increase in the lattice parameter of $ZnCr_2O_4$ may be caused by insertion of a small quantity of iron atoms from the substrate during the annealing.

To analyze the surface composition of samples, the XPS analysis was performed. Table 4 presents the movement of the binding energy (BE) of the Cr2p3, Zn2p3 and O1s peaks in the unresolved spectra recorded from the surface to depth before and after annealing of black chromium. It is seen that the surface layer of the as-deposited coating shows higher BE values than that after annealing of the sample. The shift in BE of both the Cr2p3 and Zn2p3 peaks after annealing suggests a change in the chemical state of both metals from hydroxides into oxides. This is evidenced by a shift of the O1s peak to a lower BE value and a decrease in the O/(Cr+Zn) ratio after annealing. The $Zn2p_{3/2}$ peak at BE = 1022.7 eV is assigned to $Zn(OH)_2$, whereas the peak at BE about 1021.9 eV points to the presence of ZnO [20]. The Zn2p3 peak at about 1021 eV can be due to the metallic Zn bonds formed via heating and it was emerged only in the annealed sample. The O1s peak at BE about 529.8 eV to 530.6 eV is assigned to oxygen in the oxide compounds (Cr_2O_3 and ZnO), and the peak at BE = 530.8 eV to 531.7 eV is associated with the OH^- group from the coordination environment of Cr(III) [20]. In particular, the O1s peak at 531.6 eV is due to the hydroxyl groups of $Cr(OH)_3$ and $Zn(OH)_2$. The annealed sample shows the peak at 530.0 due to the metal–oxygen bonds in ZnO and Cr_2O_3. The O1s peak positions in the spectra recorded before and after annealing suggest that the as-deposited coating is rich in hydroxides, whereas oxides become dominant after annealing of the sample. It is possible to directly observe the presence of metallic chromium in the black coating by deconvolution of the Cr2p3 spectrum [21]. The depth layer (120 nm) of the as-deposited coating was found to have four components in the Cr2p3 spectrum (Fig. 9a), the major of which (BE = 576–578 eV) may be attributed to chromium hydroxide, oxide and double oxide ($Cr(OH)_3$, Cr(OH)O, Cr_2O_3, CrO_x, $ZnCr_2O_4$) [22], whereas the minor component at BE = 574.3 eV points to the presence of metallic Cr. However, after annealing of the sample no evidence for metallic Cr was found (Fig. 9b) in the depth layer (120 nm), suggesting that the metallic phase may be converted into oxide one in the surface layers. The deconvoluted O1s spectra recorded after sputtering of top layers (120 nm) show the presence of four components for the as-deposited black chromium (Fig. 10a) and only three components after annealing of the sample (Fig. 10b). The O1s peak at BE = 529.9–530.8 eV is assigned to Cr_2O_3 and the peak at BE = 531.2–531.7 eV is attributed to $Cr(OH)_3$. It is seen that after annealing of the sample the major component shifts to a lower BE value which suggests that oxides became dominant. The high energy peak (BE = 533.8 ± 0.4 eV), which is associated with oxygen in organic fragments captured by the growing deposit, was not detected after annealing of the sample.

Table 4. **Binding energy of chromium, zinc and oxygen species in the surface layers of as-deposited and annealed black chromium and correlation of O/(Cr+Zn)**

Depth! As-deposited! 600 °C/60 min								
nm	**Cr2p3 BE (eV)**	**Zn2p3 BE (eV)**	**O1s BE (eV)**	**Correlation O (Cr+Zn)**	**Cr2p3 BE (eV)**	**Zn2p3 BE (eV)**	**O1s BE (eV)**	**Correlation O (Cr+Zn)**
0	577.97	1022.46	531.57	16.17	576.36	1021.08	530.56	3.42
15	576.87	1021.79	530.46	6.20	576.90	1021.87	530.67	2.41
45	576.87	1022.04	530.95	2.98	576.89	1022.06	530.94	2.31
120	576.90	1022.03	531.02	2.48	576.78	1021.87	530.74	2.13
270	576.92	1022.01	531.02	2.13	–	–	–	–
420	576.83	1021.94	530.90	1.88	–	–	–	–

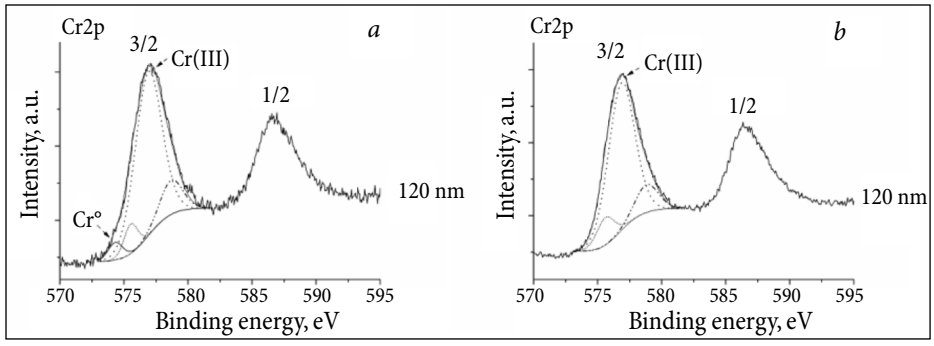

Fig. 9. Deconvoluted Cr2p3 spectra after recorded sputtering of top layers (120 nm) for as-deposited (*a*) and annealed (*b*) black chromium

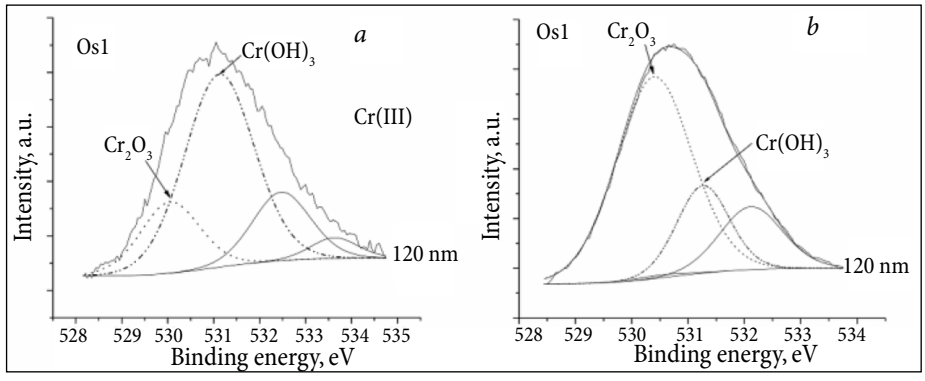

Fig. 10. Deconvoluted O1s spectra recorded after sputtering of top layers (120 nm) for as-deposited (*a*) and annealed (*b*) black chromium

The influence of annealing temperature on the optical properties of samples was studied in the solar radiation region (200–2500 nm), which is usually used for a quantitative comparison of the solar absorption of samples. It is known [23] that the spectral reflectance in the infrared (IR) region is generally dictated by the undercoating metal layer. Figure 11 shows the total (diffuse + specular) reflectance (RD) and diffuse reflectance (D) spectra measured in the UV-visible-near infrared region for black chromium before and after annealing of samples. The as-deposited coatings show much lower reflectivity than that after annealing of samples and the spectra show some specific features for each individual sample. The sample with the greatest amount of zinc shows a smooth horizontal feature of the spectral reflectance (Fig. 11c). The feeble peaks near 1 400 and 1 900 nm result from water vapour in the air and water absorbed by barium sulphate, which was used as a diffusive reflectance standard. Taking into account that the Cr–Zn layers are composed of dendrite-like agglomerations of the fine metallic particles in the matrix of dielectric materials, the low reflectivity can be attributed to the metallic

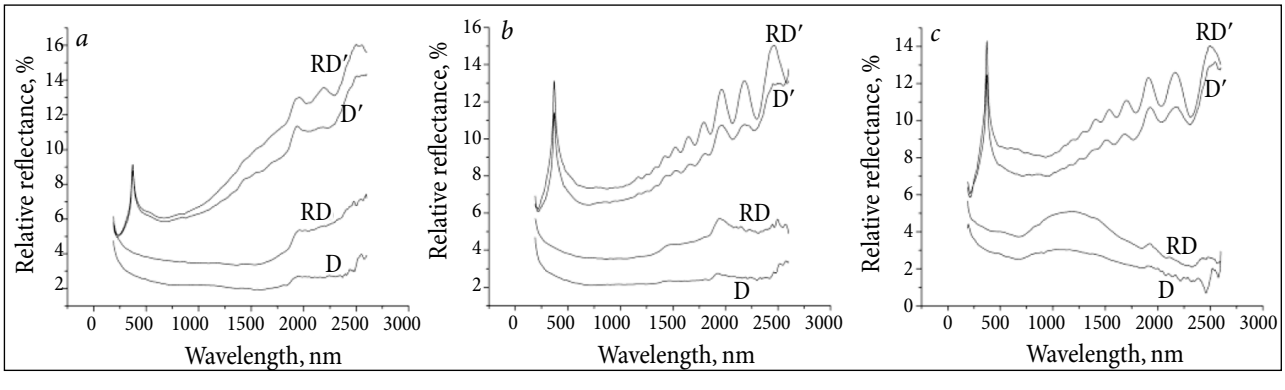

Fig. 11. The reflection spectra recorded before (D, RD) and after annealing (D′, RD′) of black chromium coatings deposited at 0.4 A cm^{-2} from Cr(III) baths containing ZnO: 5 g l^{-1} (*a*); 7.5 g l^{-1} (*b*) and 10.0 g l^{-1} (*c*)

structure which traps the light and induces multiple reflections leading to enhanced absorption due to an increased path of the light inside the material.

The reflectance spectra recorded for annealed samples differ substantially from those for as-deposited coatings. The reflectance is increased at least twofold and the spectra become similar to each other with a sharp feature at 372 nm and interference in the IR region, though for sample *a* the interference is barely observable. The reflectivity is about 6–8% over the range 500 to 1 100 nm and then considerably increases. The sharp feature at 372 nm can be explained by the localized plasmon resonance in metallic nanoparticles. Probably the agglomerations of fine metallic particles are partially destroyed (increased reflectance supports this suggestion), some of them diffuse to the oxide matrix and become isolated. The rough estimation of a criterion of the surface plasmon resonance [24] from comparison of real parts of the complex dielectric function shows that in our case the metallic Cr particles surrounded by the Cr, Zn oxide matrix satisfy the criterion of the resonance. Also the Cr–Zn layers become more homogeneous after annealing owing to which light absorption decreases and more light escapes from the material. As we know, the thickness of the Cr–Zn layers (6.5 and 4.8 μm for samples *b* and *c*, respectively), the refraction index can be estimated from the interference peaks. The calculated refraction index was found to be similar for both samples decreasing from 9 at 1 400 nm to 3 at 2 400 nm. Based on this, we assume that if the optical properties of samples *b* and *c* are similar, there is no any considerable difference in their microstructures after annealing.

The reflectance measurements were used to derive absorption [$a_w(m, p)$], that is the fraction of incident energy at a given wavelength (w) and direction (m, p) absorbed by the material. In practice absorption is an average (integrated) value. According to the literature data [17]

$$A + T + R = 1, \quad (1)$$

where A is the absorptance, T is the transmittance, R is the reflectance of the surface.

As $T = 0$ for the opaque surface, the absorptance is determined by the equation:

$$A = 1 - R. \quad (2)$$

On the average, the magnitude of the total reflectance of black chromium prepared on the steel substrate was found to be about 4% with some deviation in the near-infrared range, which depends on the percentage of zinc in black chromium. It can be said that the value of solar absorption is about 96%. However, after annealing of the samples at 600 °C the solar absorption was found to be about 92–94% in the visible range and about 84–86% in the infrared one. The analysis of the results gives an insight into the causes of degradation of the Cr–Zn coating subjected to elevated temperature (600 °C) which is very important over the lifetime of the selective solar coating. It may be concluded that the difference in the optical properties is strongly dependent on such factors as the layer microstructure, surface composition and diffusion.

CONCLUSIONS

The relationship between the microstructure and optical properties of the black Cr–Zn coating deposited on the steel substrate has been studied using as-deposited and annealed at 600 °C samples.

It was found that during the electrodeposition of black chromium from the Cr(III) bath containing ZnO the chromium solid solution in zinc of a hexagonal structure (*hcp*) may be formed along with that of zinc in chromium (*bcc*). The cross-section image of the Cr–Zn layer made it possible to reveal the presence of very small dendrite-like formations of crystalline structures in the amorphous matrix.

The annealed black chromium was found to have ZnO and $ZnCr_2O_4$ particles of a crystalline structure and a small amount of Fe_2O_3, which is the result of oxidation of the steel substrate during the annealing process. Besides, a small quantity of iron atoms from the substrate may be inserted into the $ZnCr_2O_4$ lattice in the form of the $FeCrZnO_4$ particle according to the XRD measurements.

The analysis of the near-surface layers suggests that the as-deposited black chromium is rich in hydroxides of both chromium and zinc and contains inclusions of metallic chromium, whereas after annealing of the sample oxides become dominant in the absence of metallic Cr.

The as-deposited black chromium depicts good absorptance properties for the absorption of solar energy. The increase in the reflectance of annealed samples was found to be arising from the changes in the chemical composition and structure of the deposit.

Received 28 September 2015
Accepted 5 October 2015

References

1. K. D. Lee, W. Ch. Jung, J. H. Kim, *Sol. Energy Mater. Sol. Cells*, **63**, 125 (2000).
2. P. M. Driver, R. W. Jones, C. L. Riddiford, R. J. Simpson, *Sol. Energy*, **19**, 301 (1977).
3. Y. Mastai, S. Polarz, M. Antonietti, *Adv. Funct. Mater.*, **12**, 197 (2002).
4. D. Gall, R. Gampp, H. P. Lang, P. Oelhafen, *J. Vac. Sci. Technol., A*, **14**, 374 (1996).
5. N. C. Bhowmik, J. Rahman, M. A. Alam Khan, Z. H. Mazumder, *Renew. Energy*, **24**, 663 (2001).
6. G. Zajac, G. B. Smith, A. Ignatiev, *J. Appl. Phys.*, **51**, 5544 (1980).
7. J. N. Sweet, R. B. Pettit, M. B. Chamberlain, *Sol. Energy Mater.*, **10**, 251 (1984).
8. G. B. Smith, K. Teytz, P. Hillery, *Sol. Energy Mater.*, **9**, 21 (1983).

9. G. B. Smith, G. Zajac, A. Ignatiev, J. W. Rabalais, *Surf. Sci.*, **114**, 614 (1982).
10. G. B. Smith, A. Ignatiev, *Sol. Energy Mater.*, **2**, 461 (1980).
11. G. B. Smith, P. Hillery, K. Teytz, *Thin Solid Films*, **108**, 239 (1983).
12. P. H. Holloway, K. Shanker, R. B. Pettit, R. R. Sowell, *Thin Solid Films*, **72**, 121 (1980).
13. M. Aguilar, E. Barrera, M. Palomar-Pardav, L. Huerta, S. Muhl, *J. Non-Cryst. Solids*, **329**, 31 (2003).
14. K. Shanker, P. H. Holloway, *Thin Solid Films*, **127**, 181 (1985).
15. D. Bacon, A. Ignatiev, *Sol. Energy Mater.*, **9**, 3 (1983).
16. K. D. Lee**,** *J. Korean Phys. Soc*., **51(1)**, 135 (2007).
17. M. R. Bayati, M. H. Shariat, K. Janghorban, *Renew. Energy*, **30**, 2163 (2005).
18. S. Survilienė, A. Češūnienė, R. Juškėnas, et al., *Appl. Surf. Sci*., **305**, 492 (2014).
19. C. D. Wagner, W. M. Riggs, L. E. Davis, J. F. Moulder, G. E. Muilenberg, *Handbook of X-ray Photoelectron Spectroscopy*, Perkin-Elmer, Minneapolis**,** MN, 190 (1978).
20. C. D. Wagner, A. V. Naumkin, A. Kraut-Vass, J. W. Allison, C. J. Powell, J. R. Rumble Jr., *NIST Standard Reference Database 20*, Version 3.4 (Web Version) (2003).
21. S. Survilienė, A. Češūnienė, V. Jasulaitienė, I. Jurevičiūtė, *Appl. Surf. Sci*., **324**, 837 (2015).
22. G. C. Allen, S. J. Harris, J. A. Jutson, J. M. Dyke, *Appl. Surf. Sci*., **37**, 111 (1989).
23. C. M. Lampert, J. Washburn, *Sol. Energy Mater.*, **1**, 81 (1979).
24. H. Amekura, N. Umeda, K. Kono, Y. Takeda, N. Kishimoto, Ch. Buchal, S. Mantl, *Nanotechnol.*, **18**, 395707 (6 pp) (2007).

S. Survilienė, R. Juškėnas, V. Jasulaitienė, A. Selskienė, A. Češūnienė, A. Suchodolskis, V. Karpavičienė

ATKAITINIMO ĮTAKA JUODO CHROMO DANGŲ, NUSODINTŲ IŠ Cr(III) ELEKTROLITŲ, STRUKTŪRINĖMS IR OPTINĖMS SAVYBĖMS

S a n t r a u k a

Juodo chromo danga, turinti mažą šviesos atspindžio koeficientą, buvo elektrochemiškai nusodinta ant plieno iš Cr(III) elektrolito, kurio sudėtyje yra ZnO. Ištirta, kaip aukšta temperatūra veikia dangos sudėtį, struktūrą, morfologiją ir optines charakteristikas. Šiems tyrimams atlikti buvo naudotos RSD, SEM ir EDS metodikos. Juodo chromo atspindžio koeficientas matuotas šviesos bangų ilgių intervale (190–2600 nm). Rentgenogramos parodė, kad priklausomai nuo Zn kiekio (at. %) dangos gali būti charakterizuojamos dvejopai: kietasis chromo tirpalas su cinku (*hcp* struktūros) arba kietasis tirpalas su chromu (*bcc*). Pavyzdžiai su juodo chromo danga buvo kaitinami 2 val. azoto atmosferoje 600 °C temperatūroje. Nustatyta, kad atkaitintame juodame chrome yra ZnO ir $ZnCr_2O_4$ kristalinės struktūros dendritai, nedidelis kiekis Fe_2O_3 (dėl substrato oksidacijos) ir $FeCrZnO_4$ (dėl Fe atomų įsiterpimo į $ZnCr_2O_4$ kristalinę struktūrą). REFS duomenų analizė rodo, kad prieš pavyzdžių atkaitinimą viršutiniuose dangos sluoksniuose vyrauja abiejų metalų hidroksidai su nedideliu kiekiu metalinio chromo, tačiau po dangos atkaitinimo vyrauja abiejų metalų oksidai be metalinės fazės. Optiniai matavimai parodė, kad po atkaitinimo juodo chromo absorbcinės savybės pablogėja dėl dangos cheminės sudėties ir struktūros pasikeitimo bei substrato (Fe) difuzijos į juodo chromo dangą. Šių tyrimų rezultatai patvirtina kai kurias ankstesnes išvadas ir pateikia naujos informacijos apie juodo chromo dangų gebėjimą absorbuoti saulės energiją.